Factors affecting pathogenicity of the turfgrass dollar spot pathogen in natural and model hosts

Rioux, R.A.[1¶], Stephens, C.M.[2&]., and J.P. Kerns[2&]

[1] Department of Plant Pathology, University of Wisconsin-Madison, Madison, WI, United States

[2] Department of Entomology and Plant Pathology, North Carolina State University, Raleigh, NC, United States

* Corresponding author

Email: cmsteph2@ncsu.edu (CMS)

¶ RR was the primary author. She designed, performed, and analyzed data for all experiments, and wrote the manuscript.

&CMS and JPK contributed ideas for experimentation and experimental design.

Abstract

Clarireedia sp. (formerly called *Sclerotinia homoeocarpa*), the fungal pathogen that causes dollar spot of turfgrasses, produces oxalic acid but the role of this toxin in *Clarireedia* sp. pathogenesis is unknown. In the current study, whole plant inoculation assays were used to evaluate pathogenesis of *Clarireedia* sp. in various model hosts and investigate the role of oxalic acid in dollar spot disease. These assays revealed that both host endogenous oxalate content and pathogen-produced oxalic acid influence the timing and magnitude of symptom development. In time-course expression analysis, oxalate oxidase and related defense-associated germin-like protein genes in creeping bentgrass showed strong up-regulation starting at 48-72 hpi, indicating that germin-like protein genes are most likely involved in defense following initial contact with the pathogen and demonstrating the importance of oxalic acid in *Clarireedia* sp. pathogenesis. Overall, the results of these studies suggest that oxalic acid and host endogenous oxalate content are important for pathogenesis by *Clarireedia* sp. and may be associated with the transition from biotrophy to necrotrophy during host infection.

KEYWORDS: *Sclerotinia homoeocarpa*, *Clarireedia* sp., *Rutstroemiaceae,* dollar spot, creeping bentgrass, oxalic acid

Introduction

Clarireedia sp. (formerly called *Sclerotinia homoeocarpa*) cause dollar spot in turfgrass, which is one of the most important diseases of amenity turfgrasses worldwide [1]. Despite the previous name *Sclerotinia homoeocarpa,* recent literature confirmed that this pathogen is not a species of *Sclerotinia* or a member of any known genus within the *Rutstroemiaceae* [2]. Renaming and correct taxonomic placement of *Sclerotinia homoeocarpa* has resulted in the establishment of a new genus described as *Clarireedia* gen. nov. [2]. A total of four distinct pathogenic species that cause dollar spot have been characterized within this genus, with *C. jacksonii* and *C. monteithiana* primarily infecting C3 and C4 grasses in North America, respectively [2]. Isolates evaluated in the current study were sampled from both C3 and C4 grasses. Therefore, the *C. jacksonii/C. monteithiana* are referred to as *Clarireedia* sp. in this text. *Clarireedia* sp. have a broad host range that spans five plant families [2] and includes economically and ecologically important plants, such as switchgrass [3], perennial peanut [4], and tufted bulrush [5].

Dollar spot is of particular concern in golf course settings because the sunken, silver dollar-sized spots of diseased turf from which this disease earns its name are aesthetically unappealing and may negatively affect ball roll. Conditions favoring dollar spot development are broad. The fungus can grow and cause disease at temperatures ranging from 14-35°C, if relative humidity remains above 70% [1]. As a result, successful dollar spot management requires periodic fungicide applications throughout the growing season, making dollar spot the most economically important disease of turf worldwide [1, 6, 7].

Popular turfgrass species that are prone to dollar spot, particularly creeping bentgrass (*Agrostis stolonifera,* L.), have complex polyploid genomes and are outcrossing which make

69 genetic characterization of dollar spot resistance difficult [8]. To date, only a single study exists
70 comparing global gene expression among inoculated and non-inoculated creeping bentgrass plants
71 [9] and dollar spot resistance has been identified on only a few major quantitative trait loci [10].
72 Moreover, the size of individual turfgrass plants makes it difficult to manipulate and visually assess
73 disease phenotypes. An acceptable model host would provide a much-needed tool for molecular
74 and phenotypic characterization of *Clarireedia* sp./host interactions and may be applicable to other
75 turfgrass pathogens.

76 The vast array of genetic resources for *Arabidopsis thaliana* make it a natural choice as a
77 model host for any pathosystem. Further, *A. thaliana* has been successfully used in a number of
78 studies on pathogenicity of *Sclerotinia sclerotiorum* (*Ss*) and *Botrytis cinerea*, both of which
79 belong to the same fungal order as *Clarireedia* sp. [11, 12, 13, 14, 15, 16]. However, *S.*
80 *sclerotiorum* and *B. cinerea* are predominantly pathogens of dicots while *Clarireedia* sp. prefer
81 monocot hosts, indicating that a monocot model host may be more suitable for studies of
82 *Clarireedia* sp. pathogenesis. Rice is a forerunner in cereal genetic resources [17], but less closely
83 related to creeping bentgrass and other major turfgrass species than *Brachypodium distachyon*,
84 barley, or wheat [18, 19]. Studies of host/pathogen interactions and generous genetic resources are
85 available for all three of these plants, indicating their potential utility as model hosts for
86 *Clarireedia* sp. Consequently, one of the objectives of the present research was to compare
87 *Clarireedia* sp. pathogenesis between these five model hosts and the natural host creeping
88 bentgrass.

89 Identifying pathogenicity mechanisms is important for understanding pathogenesis in
90 *Clarireedia* sp. Previously, researchers showed that this pathogen produces oxalic acid (OA) [12].
91 OA is a common phytotoxin and is produced by many important plant pathogens, particularly

92 those in the *Sclerotiniaceae* family [20], to which *Clarireedia* sp. are closely related. *S.*
93 *sclerotiorum*, a polyphagous necrotrophic plant pathogen with more than 400 hosts [6, 7] relies
94 heavily on production of OA for successful pathogenesis. While the role of OA in *Ss* pathogenesis
95 has been extensively studied [21, 15, 14, 7, 22], the function of OA in *Clarireedia* sp. pathogenesis
96 is not clear.

97 Differences among the *Clarireedia* sp. and *S. sclerotiorum* host ranges indicate that these
98 pathogens use OA in disparate ways during host colonization. *Clarireedia* sp. primarily infect
99 monocot species within the family *Poaceae* [2]. Conversely, *S. sclerotiorum* infects a broad range
100 of dicot species, but is not considered a pathogen on most monocots. Many grass species have
101 oxalate oxidases that degrade OA, preventing successful infection by *Ss* [23, 24]. Transformation
102 of dicot hosts with grass oxalate oxidase genes confers partial resistance to *Ss* [26, 27, 28].
103 Consequently, if OA is an important pathogenicity factor for *Clarireedia* sp., this fungus must use
104 the phytotoxin in a manner that allows it to circumvent or overcome oxalate oxidase-mediated
105 plant defenses. Both oxalate oxidase activity [9] and up-regulation of oxalate oxidase encoding
106 genes occur during *Clarireedia* sp. infection of creeping bentgrass [29], indicating that OA is
107 produced *in planta* during host colonization. A better understanding of the role of OA in host
108 colonization by *Clarireedia* sp. and host oxalate oxidase-mediated defenses against *Clarireedia*
109 sp. may contribute to novel disease management strategies.

110 Based on these observations, the objectives of the present research were to: 1) Investigate
111 the infection process of *Clarireedia* sp. in creeping bentgrass and various model host systems and
112 2) determine the role of OA in *Clarireedia* sp./host pathogenesis.

Materials and methods

Biological materials.

Plant materials.

Monocots (S1 Table) were grown from seed and maintained in a growth room with a 14 h light period at 25±2°C and 10 h dark period at 22±2°C. *Arabidopsis thaliana* and *Nicotiana benthamiana* were grown under similar conditions, except growth chamber conditions were modified to an 18 h day-length and constant temperature of 26±2°C.

Fungal materials.

Fungal isolates (S2 Table) were maintained on potato dextrose agar (PDA) under ambient temperature (22±2°C) in growth chambers with a 24 h dark period and transferred weekly to maintain viability. For long term isolate storage, mycelia were allowed to colonize sterile filter paper disks on PDA, air dried, placed in glass vials, and stored at -80°C.

Inoculation assays and disease rating.

Monocots were inoculated using the previously described parafilm sachet method [30]. The exact method used differed slightly with host species (S1 Fig). Dicots were inoculated by placing an agar plug mycelia side down on a fully expanded leaf surface. Flats containing inoculated dicots were covered with plastic domes to promote relative humidity >90%. Parafilm alone maintained high relative humidity for monocot inoculations and domes were not needed. Four-day-old cultures of *Clarireedia* sp. were used for all plant inoculations. Control plants were mock-inoculated with agar plugs from fresh PDA plates.

Symptom severity was rated every 24 h using a rating scale modified from the Horsfall-Barratt scale (S3 Table) [31]. This method allowed for direct comparison of symptom severity between species with diverse physical characteristics and symptom phenotypes. To prevent the possibility of rater-to-rater variability all symptom severity ratings were made by the same individual.

Inoculation experiments were repeated three times with three replicates of each treatment or treatment combination per experimental repetition (n=9). Data were analyzed with experimental repetition treated as a random blocking factor and blocks within each repetition treated as a random factor nested within experimental repetition. Plant species and fungal isolate were both considered fixed effects.

Trypan blue staining and microscopy.

Inoculation and sample collection for all plant hosts and *Clarireedia* sp. isolates were performed in parallel. Scissors were used to excise plant material surrounding the site of inoculation and individual tissue samples were placed in 2mL microcentrifuge tubes. Staining and clearing of tissues were performed as previously described [32]. All samples were visualized with an Axio Scope.A1 compound microscope (Zeiss, Thornwood, NY). Images were captured with an AxioCam MRc camera and processed with accompanying AxioVision Real 4.7.1 imaging software (Zeiss, Thornwood, NY). A minimum of three samples were examined for each time-point, isolate, and host combination.

Whole plant oxalate quantification.

153 Plants for oxalate quantification were inoculated as previously described. For fresh plant
154 samples, 0.25 g of tissue were ground in liquid nitrogen with a mortar and pestle then added to a
155 15 mL centrifuge tube containing 4 mL of 0.2 M KH_2PO_4 buffer (pH 6.5) [33]. Tubes containing
156 ground plant tissue were placed on their sides on an incubator shaker table and mixed overnight
157 with constant gentle shaking at 90 revolutions per minute at room temperature (22±2°C). The
158 following day, 2 mL of the liquid portion from each sample tube was transferred to a fresh 15 mL
159 centrifuge tube and mixed with 2 mL of freshly prepared oxalate quantification kit sample diluent
160 (Trinity Biotech, Jamestown, NY). The remainder of the oxalate assays were performed according
161 to the manufacturer's instructions (Trinity Biotech, Jamestown, NY). Oxalate content was
162 quantified based on absorption at 590 nm with a UV/Vis spectrophotometer (Beckman Coulter,
163 Brea, CA). A 0.5 mmol oxalate standard was included in each run.

164 Due to the high volume of samples in time-course oxalate studies, samples for this assay
165 were harvested, weighed, flash frozen in liquid nitrogen, and stored at -80°C until use. Pilot studies
166 indicated that flash freezing did not affect oxalate content in comparison with samples processed
167 when fresh. Frozen samples were lightly ground in liquid nitrogen with a mortar and pestle, then
168 transferred to Lysing Matrix A FastPrep tubes (MP Biomedicals, Santa Ana, CA) with 1.5 mL
169 KH_2PO_4 buffer and ground in a FastPrep at 6.0 m/s for 40 s (MP Biomedicals, Santa Ana, CA).
170 Homogenized samples were poured into 15 mL centrifuge tubes and mixed with 1.5 mL sample
171 diluent. Oxalate quantification was then performed as previously described.

172 Germin-like protein gene expression analysis.

173 Pots of one-week-old creeping bentgrass turfgrass cultivars '96-2' and 'Focus' were
174 inoculated with two agars plugs colonized with *Clarireedia* sp. mycelia and covered to maintain

175 humidity >90%. Cultivars '96-2' and 'Focus' were chosen for their low and high resistance to
176 dollar spot in field trials, respectively (http://www.ntep.org). The experiment was arranged as a
177 two treatment (inoculated and mock-inoculated) by two cultivar ('96-2' and 'Focus') factorial
178 within a randomized complete block design with four replications. Pots were resampled at 0, 24,
179 48, 72, and 96 hpi by harvesting 100 mg of tissue from the area surrounding the site of inoculation,
180 removing roots and leaf blade tips, flash freezing in liquid nitrogen, and storing at -80°C until use.

181 Samples for RNA extraction were ground with a mortar and pestle in 500 µL frozen Trizol
182 reagent then transferred to 2 mL microcentrifuge tubes containing 500 µL Trizol reagent. RNA
183 extraction was then performed with the Trizol Plus RNA Purification Kit including the optional
184 on-column DNase step according to the manufacturer's instructions (Life Technologies, Grand
185 Island, NY). RNA quality was assessed with an Experion Automated Electrophoresis Station using
186 the Experion RNA StdSens analysis kit (BioRad, Hercules, CA) and yield was quantified with an
187 ND-1000 spectrophotometer (Nanodrop, Wilmington, DE). Samples were stored at -80°C until
188 further use.

189 Synthesis of cDNA and RT-qPCR were performed according to the specifications of the
190 MIQE guidelines. Prior to cDNA synthesis, a no cDNA control RT-qPCR run was performed on
191 pure RNA to confirm the absence of contaminating genomic DNA. RNA samples confirmed as
192 free of genomic DNA were diluted to equivalent concentrations and subjected to cDNA synthesis
193 with iScript cDNA Synthesis Kit according to the manufacturer's instructions (BioRad, Hercules,
194 CA). All cDNA synthesis reactions for a single time-point were performed simultaneously to
195 decrease any inherent variability in the synthesis process. cDNA quality was assessed by
196 comparing Cq values for potential reference genes and reference genes were selected using
197 BestKeeper Software [34]. Creeping bentgrass actin (ACT7) and glyceraldehyde phosphate

198 dehydrogenase (GAPDH) genes were selected as stable reference genes for all time-points in both
199 cultivars.

200 Primers for RT-qPCR were designed from publicly available creeping bentgrass EST
201 sequences with Primer3 primer design software (http://www.genome.wi.mit.edu/genome_
202 software/other/primer3.html; S4 Table) and validated by generating efficiency curves from a
203 dilution series of cDNA pooled from all time-points. For RT-qPCR, cDNA samples were diluted
204 10-fold and a final volume of 8 µL cDNA was used in each of three 20 µL technical replicates per
205 reaction, along with 10 µL SsoFast EvaGreen Supermix (BioRad, Hercules, CA), 0.3 µM of each
206 primer, and nuclease free water. All reactions were run in hard-shell skirted 96-well plates with a
207 white top and clear wells and sealed with Microseal 'B' adhesive film (BioRad, Hercules, CA). A
208 CFX-96 detection system (BioRad, Hercules, CA) was used for quantification. PCR conditions
209 were 98°C for 2 m; 40 cycles of 98°C for 2 s and 55°C for 5 s; followed by a dissociation curve
210 with 80 cycles starting at 70°C for 10 s and increasing in 0.2°C increments per cycle. The
211 dissociation curve was used to detect primer-dimers and amplification of a single product within
212 the CFX detection system software (BioRad, Hercules, CA).

213 To calculate relative expression of target genes, transcript abundance was internally
214 normalized to the two reference genes (actin and elongation factor 1-α) that were included on each
215 experimental plate using the formula $2^{\Delta Cq(\text{target-reference})}$ [35]. Relative expression ratios of target
216 genes were then calculated using a method based on the previously described $2^{-\Delta\Delta Cq}$ method [35,
217 36, 37]. Briefly, normalized target gene Cq values for infected plant tissue were divided by a
218 calibrator value, which was calculated by averaging the normalized Cq values for all uninfected
219 96-2 samples from the same time point [35]. This method allowed for comparison between all
220 treatment levels at each time-point. Statistical analysis was performed on resulting relative

221 expression ratios using the proc mixed procedure in SAS v.9.3 (SAS Institute, Cary, NC).
222 Orthogonal contrasts were used to compare relative expression ratios between mock-inoculated
223 and inoculated samples within each cultivar and between the inoculated samples of the two
224 cultivars.

225 ## Statistical analysis.

226 Data analysis was performed using the MIXED, generalized linear mixed model
227 (GLIMMIX), and regression (REG) procedures in SAS version 9.3. Initial models were fit
228 including all random factors and interactions with fixed factors. Model fitting criteria (Akaike's
229 Information Criterion) were then used to remove random factors and interactions not contributing
230 to variability in order to identify the best model for each data set. Visual analysis of residual plots
231 and output from PROC UNIVARIATE were used to assess normality of the data. Data were
232 transformed as necessary to best approximate the normal distribution using the DIST= option in
233 PROC GLIMMIX. Reported values were back-transformed using the ILINK option. The ANOVA
234 F-test was used to determine contributions of fixed factors to variability in the measured response
235 variable(s). Additionally, pre-planned orthogonal contrasts were used to compare between specific
236 fixed factors.

237 Use of the symptom severity rating scale resulted in data with a non-normal distribution
238 that could not be corrected through common data transformations available within PROC
239 GLIMMIX. Consequently, a Friedman's two-way analysis for block designs was employed [38].
240 For each experimental repetition, the symptom severity for each data point (species by treatment)
241 was ranked within blocks previously defined during experimental set-up. The resulting ranks were
242 assessed for normality and agreement between experimental repetitions. The rank data from each

experiment repetition was then pooled and analysis of variance was performed with the rank output as the response variable and both repetition and block(repetition) as random factors.

Results

Characterization of the *Clarireedia* sp. infection process on natural and model hosts.

Microscopic characterization of infection at various time-points following inoculation was similar regardless of host (Fig 1). As early as six hours-post inoculation, *Clarireedia* sp. hyphae were observed growing along cell walls (Fig 1A) and initiating host penetration through infection pegs (Fig 1A) and stomata (Fig 1B). This resulted in extensive colonization of host tissue, particularly xylem, shortly following inoculation (Fig 1C-E). Host cell penetration and colonization continued for at least 72 h. Dead host cells, as indicated by trypan blue staining, were observed at minimum of 48 hrs after inoculation (Fig 1J-K). Differences in the infection process were not observed with the four *Clarireedia* sp. isolates used in this study.

Fig 1. Microscopic analysis of plant foliar tissue colonization by *Clarireedia* sp. In-tact plants were inoculated and plant samples were taken by excising the area around the site of inoculation. All samples were cleared of chlorophyll and stained with 0.01% trypan blue. Host penetration was observed as early as 6 hpi and included: **A)** Growth along cell walls and formation of infection pegs (arrowheads) projecting directly into host tissue; shown in creeping bentgrass. **B)** Direct penetration through stomata; shown in barley and **C)** Extensive colonization of host tissue with an affinity for vascular tissue; shown in barley. At 12 to 24 hpi fungal hyphae continued to grow along cell walls and form penetration pegs into vascular tissue, as observed in **D)** Creeping

bentgrass at 12 hpi **E)** Wheat at 24 hpi and **G)** Rice at 24 hpi. **F)** *Clarireedia* sp. protruding from a stomate in *Arabidopsis thaliana* tissue colonized by fungal mycelia. **H)** Appressorium (arrowhead) formed by a *Clarireedia* sp. hypha on barley at 96 hpi. **I)** Extensive host cell death, as indicated by trypan blue staining outside of fungal hyphae, was not observed until 4-7 dpi regardless of host. **J)** Extensive cell death 7 dpi inoculation of *Brachypodium distachyon* with *Clarireedia* sp. **K)** Extensive cell death outside of host vascular tissue at 7 dpi in wheat. Images are representative of similar observations made for all hosts and *Clarireedia sp.* isolates used in this study.

Symptoms of *Clarireedia* sp. infection were similar in monocot hosts, but differed in the dicot host *Arabidopsis thaliana* (Fig 2). Inoculation of creeping bentgrass plants resulted in bleaching and necrosis of the inoculated leaf area (Fig 2F). Within this area, individual leaf blades with hourglass shaped lesions of white-gray tissue surrounded by reddish-brown borders were identified (Fig 2E). Similar lesions were observed on the four model monocot hosts (Fig 2A-D). Occasionally, complete wilting of infected leaves was observed, particularly in the later stages of infection. Symptoms on *A. thaliana* began as water-soaked lesions, with the affected areas eventually wilting. These lesions were visually distinct from necrotic lesions typically observed in studies of *A. thaliana* inoculated with the related pathogen *Ss* [15]. The petiole of the inoculated *A. thaliana* leaf would become necrotic, constricted, and the symptomatic leaf would often separate from the plant following severe infection.

Fig 2. Symptoms produced by *Clarireedia* sp. on natural and model host plants. *Clarireedia* sp. infected and produced visible symptoms on all host plants. Similar symptoms were observed on **A)** *Brachypodium distachyon* **B)** Wheat **C)** Barley and **D)** Rice. These symptoms included light tan to white lesion with reddish brown borders and resembled those observed on **E)** Creeping

bentgrass, a natural host. **F)** Creeping bentgrass stand symptoms resulting from our parafilm sachet inoculation method looked visibly similar to symptoms observed in the field. **G)** Foliar symptoms observed on *Arabidopsis thaliana* were distinct from those observed on monocot hosts and were characterized by water soaking and tissue collapse.

Analysis of area under the disease progress curve (AUDPC) values revealed a significant effect of species, but not isolate or isolate x species interaction based on a simple two-way ANOVA F-test *(P*=0.01) (Fig 3A). In particular, AUDPC values were different between rice and creeping bentgrass according to a Dunnett's test comparing mean AUDPC values for species (*P*=0.0043). Overall symptom severity in time-course assays was only affected by host species at 48 hpi *(P*=0.03), when symptoms began to rapidly develop in *B. distachyon* and *O. sativa* (Fig. 3B). However, greater symptom severity was observed in rice at 48, 72, and 96 hpi (*P*<0.05) and in *B. distachyon* at 48 hpi (*P*=0.01) when compared specifically to creeping bentgrass. No additional differences in symptom severity between creeping bentgrass and other species were found. Throughout these experiments, symptom severity on mock-inoculated controls remained at or near zero.

Fig 3. Symptom severity of *Clarireedia* sp. infection on natural and model hosts. All plants were inoculated in the same time in a split-plot RCBD with host as the whole-plot factor and *Clarireedia* sp. isolate as the sub-plot factor. Three experimental repetitions were conducted and treated as a random blocking factor in experimental analyses. Blocks within experimental repetitions were considered random factors nested within repetition. Host, isolate, and host x isolate interaction were fixed effects. **A)** AUDPC for each *Clarireedia* sp. isolate on the six host plants. Colored bars represent four different *Clarireedia* sp. isolates. P-values presented are from a two-way ANOVA with $\alpha = 0.05$. Asterisks indicate significant difference from the natural host

creeping bentgrass (AS) based on a Dunnett's test with $\alpha = 0.05$. Only the AUDPC for rice (OS) differed from that of creeping bentgrass. N≥9 for each species*isolate combination. **B)** Time-course progression of infection by *Clarireedia* sp. on all host species. The black asterisk indicates an overall significant effect of species on symptom severity at 48 hpi, as assessed by one-way ANOVA. Blue and orange asterisks indicate significant differences between rice and *B. distachyon* (BD), respectively, and creeping bentgrass at the corresponding time-points based on analysis with Dunnett's test. N≥30 for each species. Abbreviations for both figures are as follows: AS=*Agrostis stolonifera* (creeping bentgrass); AT=*Arabidopsis thaliana*; BD=*Brachypodium distachyon*; HV=*Hordeum vulgare* (barley); OS=*Oryza sativa* (rice); and TA=*Triticum aestivum* (TA). For significance codes, *=P≤0.05; **=P≤0.01; ***=P≤0.001. All error bars represent ± one standard error of the mean.

Relationship between host endogenous oxalate content and symptom development.

To explore the relationship between *Clarireedia* sp. pathogenicity and OA, the oxalate content of plants inoculated with *Clarireedia* sp. or mock-inoculated with PDA was compared. A positive relationship between oxalate content and symptom severity was detected in creeping bentgrass, barley, and wheat, with R^2 values ranging from 0.33 to 0.52 (Fig 4). The relationship between oxalate content and symptom severity in rice and *B. distachyon* was also positive, but lower than for the other species (R^2 values of 0.10 and 0.01, respectively). A negative relationship between oxalate content and symptom severity was observed in *Arabidopsis thaliana*; however, correlation was low. Endogenous oxalate content of the six species differed significantly

331 (*P*<0.0001) and comparisons against creeping bentgrass revealed that both rice and *B. distachyon*
332 had higher oxalate levels (*P*<0.0001; Fig 4).

333 **Fig 4. Correlation between host endogenous oxalate content and symptom severity. A)**
334 Endogenous oxalate content of all host species used in this study. Asterisks indicate significant
335 difference from creeping bentgrass (AS) at the α=0.05 level using Dunnett's test. Error bars
336 represent ± one standard error of the mean. **B)** Correlation between oxalate content and symptom
337 severity of *Clarireedia* sp. infection were fit a linear regression model for creeping
338 bentgrass/*Agrostis stolonifera* (As), *Arabidopsis thaliana* (At) , *Brachypodium distachyon* (Bd),
339 barley/*Hordeum vulgare* (Hv), rice/*Oryza sativa* (Os), and wheat/*Triticum aestivum* (Ta). All
340 regression equations, R^2, and P-values were obtained from models fit with SAS proc reg. For
341 significance codes, *=P≤0.05; **=P≤0.01; ***=P≤0.001. All error bars represent ± one standard
342 error of the mean.

343 A time-course experiment was performed to compare symptom severity and oxalate
344 content between *Clarireedia* sp.-inoculated and mock-inoculated plants during the progression of
345 infection. Creeping bentgrass was selected to represent species with low oxalate content and *B.*
346 *distachyon* was selected to represent species with high oxalate content. *B. distachyon* was selected
347 over *O. sativa* because symptom severity and genetics were more similar to creeping bentgrass
348 [18]. Oxalate content in *Clarireedia* sp.-inoculated plants gradually increased over time and
349 paralleled the development of symptoms (Fig 5A). Oxalate content in mock-inoculated plants
350 remained low throughout the experiment. Significant differences between the oxalate content in
351 *Clarireedia* sp. and mock-inoculated creeping bentgrass developed at 48 hpi (*P*=0.004) and 120
352 hpi (*P*<0.0001). Conversely, oxalate content of inoculated and mock-inoculated *B. distachyon*
353 plants remained relatively stable over time (Fig 5C). The oxalate content of inoculated and mock-

354 inoculated *B. distachyon* only differed significantly at 120 hpi (p=0.003). Oxalate content
355 correlated to symptom severity in both hosts (*P<0.0001*), but 75% of the variability in symptom
356 severity was explained by oxalate content in creeping bentgrass, compared to only 28% in *B.*
357 *distachyon*.

358 **Fig 5. Time-course for the relationship between symptom severity and oxalate content in**
359 **creeping bentgrass and *Brachypodium distachyon.* A)** Time-course of symptom severity and
360 oxalate content in creeping bentgrass. Asterisks indicate difference between oxalate content in
361 *Clarireedia* sp. and mock-inoculated plants by one-way ANOVA with a cut-off value of α=0.05.
362 Errors bars represent ± one standard error of the mean. **B)** Scatter plot showing the correlation
363 between oxalate content and symptom severity for creeping bentgrass. Regression line calculated
364 from simple linear regression in SAS proc reg. **C)** Time-course of symptom severity and oxalate
365 content in *B. distachyon*. Asterisks indicate difference between oxalate content in *Clarireedia* sp.
366 and mock-inoculated plants by one-way ANOVA with a cut-off value of α=0.05. Errors bars
367 represent ± one standard error of the mean. **D)** Scatter plot showing the correlation between oxalate
368 content and symptom severity for *B. distachyon*. Regression line calculated from simple linear
369 regression in SAS proc reg. For significance codes, *=P≤0.05; **=P≤0.01; ***=P≤0.001. All error
370 bars represent ± one standard error of the mean.

371 To further elucidate the influence of pathogen-produced OA relative to plant endogenous
372 oxalate content on symptom development in creeping bentgrass and *B. distachyon*, the
373 aggressiveness of *Clarireedia* sp. isolates producing varying levels of OA in culture was compared
374 (Fig 6). Isolates A1421, HE10G19, and ML75 produced high, low, and moderate amounts of OA,
375 respectively, based on acidification of bromophenol blue amended medium assays (Fig S2) [39].
376 Orthogonal contrasts were used to compare symptom severity between HE10G19 (low OA prod)

and the remaining two isolates at each time point (Fig 6). On creeping bentgrass, aggressiveness of isolates differed at 72 hpi. From this point on, HE10G19 was less aggressive than the other two isolates ($p \leq 0.05$; Fig 6B). Aggressiveness among the *Clarireedia* sp. isolates did not vary on *B. distachyon* (Fig 6C).

Fig 6. Progression of infection on creeping bentgrass and *Brachypodium distachyon* by *Sclerotinia homoeocarpa* isolates with varying oxalic acid production capacities. Isolates producing high, moderate, and low amounts of oxalic acid were selected based on their ability to produce a color change in pH indicator-amended media (S2 Fig). In line graphs, red, green, and blue lines indicate isolates with high, moderate, and low oxalic acid production abilities, respectively. Creeping bentgrass and *B. distachyon* experiments were performed in tandem. Values shown in these graphs represent the means from the three experimental repetitions. **A)** Time-course of symptom development and **B)** AUDPC of symptom severity on creeping bentgrass. **C)** Time-course of symptom development and **B** AUDPC of symptom severity on *B. distachyon.* Asterisks in **A** represent a significant effect of isolate in one-way ANOVA with $\alpha=0.05$. P-values in **B** were obtained through orthogonal contrasts comparing the AUDPC means between the isolates indicated. No difference between isolates was detected for *B. distachyon*. For significance codes, *=P≤0.05; **=P≤0.01; ***=P≤0.001. All error bars represent ± one standard error of the mean.

Comparison of oxalate oxidase expression in creeping bentgrass cultivars.

A previous study determined various germin-like protein (GLP) genes, including oxalate oxidases, were some of the most up-regulated genes in the dollar spot susceptible cultivar 'Crenshaw' 96 hpi with *Clarireedia* sp. [29]. In the present study, RT-qPCR was used to compare

399 the expression of oxalate oxidase and other germin-like protein genes between cultivars considered
400 resistant and susceptible to *Clarireedia* sp. Four genes of interest were selected for RT-qPCR
401 analysis of expression through sequence alignment and phylogenetic analysis of creeping
402 bentgrass ESTs and known GLP genes from barley, rice, and *B. distachyon* (S3 Fig). Expression
403 was tested by extracting total RNA from four independent pots of *Clarireedia* sp.-inoculated or
404 mock-inoculated resistant and susceptible creeping bentgrass cultivars. All four of these genes
405 were up-regulated in both resistant and susceptible cultivars by 96 hpi in *C. Clarireedia* sp.-
406 inoculated versus mock-inoculated control plants (Figs 7 and S3). The oxalate oxidase gene,
407 AST_798, was up-regulated in the susceptible cultivar at 48, 72, and 96 hpi. Expression of
408 AST_798 was stronger in the susceptible cultivar when compared to the resistant cultivar 48 and
409 72 hpi. AST_798 was only up-regulated in the resistant cultivar at 96 hpi (Fig 7A). Similarly,
410 AST_854, a creeping bentgrass gene grouping with defense-associated GLP genes from barley
411 and rice in phylogenetic analysis, was up-regulated in the susceptible cultivar at 72 and 96 hpi, but
412 only at 96 hpi in the resistant cultivar (Fig 7B). Similar expression patterns were observed for two
413 more creeping bentgrass GLP genes that did not group with known defense-associated GLPs in
414 phylogenetic analysis (S3 Fig).

415 **Fig 7. Time-course expression of oxalate oxidase and another germin-like protein gene in**
416 **resistant and susceptible creeping bentgrass cultivars. A)** Time-course expression of the creeping
417 bentgrass oxalate gene AST_798. **B)** Time-course expression for the creeping bentgrass GLP GER4 subfamily
418 gene AST_854. Relative expression ratios shown were normalized the constitutively expressed creeping
419 bentgrass ACT7 reference gene. Similar results were obtained with the creeping bentgrass GAPDH gene. In the
420 legend for both **A** and **B**, 'S' and 'R' represent the 'susceptible' and 'resistant' cultivar, respectively; 'Sh' and
421 'PDA' indicate '*Clarireedia* sp.-inoculated' and 'PDA mock-inoculated' samples, respectively. Orthogonal
422 contrasts were used to compare relative expression ratios between specific treatment pairs at the α=0.05 level.

Black asterisks indicate a significant difference between relative expression ratios for the *Clarireedia* sp.-inoculated resistant and susceptible cultivar; blue asterisks indicate a significant difference the *Clarireedia* sp. and mock-inoculated samples for the susceptible cultivar; red asterisks indicate a significant difference between the *Clarireedia* sp. and mock-inoculated control for the resistant cultivar. For significance codes, *=P≤0.05; **=P≤0.01; ***=P≤0.001. All error bars represent ± one standard error of the mean.

Discussion

A primary objective of the present research was to identify a host species for use as a model system to study *Clarireedia* sp. pathogenesis and host resistance. The lack of a significant species by isolate interaction in this research supports previous findings in turfgrass hosts that indicate a lack of race specificity in *Clarireedia* sp./host interactions [10]. Therefore a few model host cultivars or accessions with high and low resistance to dollar spot disease could be used to dissect molecular and physiological aspects of host resistance to this pathogen. We detected differences in disease severity and symptom development between species, indicating that not all are equally suited as a model system for *Clarireedia* sp. and that *A. thaliana* is not a suitable model host for *Clarireedia* sp. The correlation between symptom severity and endogenous oxalate was an unexpected finding. Model hosts with varying levels of endogenous oxalate content may be useful further studies of *Clarireedia* sp./host interactions and how they are affected by endogenous host oxalate levels. Soybean cultivars [40] and spinach varieties [41] differ in oxalate content in the field suggesting natural variation in oxalate levels is common in plant species and should be readily identifiable in a chosen model host system. We are unaware of previous reports that plant endogenous oxalate levels influence resistance to fungal pathogens; however, oxalate is known to influence resistance to herbivory by some insects [42, 43].

To our knowledge, a correlation between host endogenous oxalate content and susceptibility to *Clarireedia* sp. has not previously been demonstrated for creeping bentgrass or any other turfgrass species. Plants produce and use oxalate for a variety of purposes, including defense, pH regulation, osmoregulation, and calcium homeostasis [44] Thus, oxalate content can vary widely between cultivars and environments. Correspondingly, resistance to dollar spot is inherited quantitatively and largely dependent upon environmental conditions [45, 46, 47, 10]. It is possible that oxalate content contributes to dollar spot resistance and this is a hypothesis that should be assessed in cultivars with varying levels of resistance to dollar spot disease.

In addition to genetic differences in creeping bentgrass cultivar oxalate content, management and environmental factors could also be used to alter this host characteristic. It has been reported that fertilizers high in ammonium content and low in nitrate are most effective at suppressing dollar spot in field trials [48]. This is of note because specific forms of nitrogen, in particular nitrate, can affect plant oxalate levels [44]. Promotion or reduction of turfgrass oxalate content could occur in response to different fertilization regimes and suggests a novel means by which nutrient management could be used to manage dollar spot. Further studies in the both the field and lab are needed to better understand the relationship between creeping bentgrass cultivar oxalate content and dollar spot resistance. Additionally, studies that investigate the effects of cultural practices, such as fertilization, on both dollar spot resistance and plant oxalate content will be useful in identifying best management practices for dollar spot suppression. Due to the correlative nature of these studies, it is also possible that it is not the oxalate content specifically that determines the outcome of the host/pathogen interaction but related factors such as foliar pH or pH within the plant.

Germin-like proteins are considered an important part of grass basal defense mechanisms [10, 49]. Consequently, the slow increase in expression of oxalate oxidase and other GLP genes in this study was unexpected. Orshinsky et al. [29] also found strong induction of GLP genes in creeping bentgrass 96 hpi inoculation with *Clarireedia* sp. Interestingly, expression of these genes in creeping bentgrass parallels the timing of symptom appearance and increased more rapidly in the susceptible cultivar compared to the resistant cultivar in this study. One possible reason for the delayed expression of host oxalate oxidase genes is that they are activated in the plant as *Clarireedia* sp. transitions from biotrophy to necrotrophy following early stages of pathogenesis. This hypothesis corresponds with our microscopic examinations of the *Clarireedia* sp. infection process, which demonstrated hyphal growth within host tissue prior to cell death. Alternatively, oxalate oxidase and other GLP genes may be expressed by creeping bentgrass only after detection of pathogen-produced OA. *Brassica napus* GLP genes are induced as early as 6 hpi with *S. sclerotiorum* but it is unclear if expression is related to detection of OA or other signs of pathogen infection [51]. Transient induction of GLP gene expression could have occurred at time-points before the 24 h initial sample collection in this study. Other components of experimental design such as age of the host or tissue collection timing post inoculation could have interfered with our ability to detect changes in gene expression at early time points. Functional studies with plants overexpressing or lacking oxalate oxidase and other GLP genes will help to better identify the importance of these genes in host resistance to *Clarireedia* sp.

Sclerotinia sclerotiorum isolates deficient in OA production are hypovirulent or non-pathogenic [39, 52]. Similarly, hypovirulent isolates of the chestnut blight fungus, *Cryphonectria parasitica*, produce lower amounts of OA *in vitro* than their virulent counterparts [53]. In this research, we found that a *Clarireedia* sp. isolate deficient in OA production had decreased

aggressiveness on creeping bentgrass but not on *B. distachyon* (Fig 6), indicating that OA contributes to aggressiveness but is not a pathogenicity determinant for *Clarireedia* sp. and that *Clarireedia* sp. with reduced OA production may infect more efficiently on hosts with higher endogenous oxalate content. Similarly, the symptoms observed on *A. thaliana* were visibly distinct from those observed on monocots and no increase in oxalate content was found in symptomatic *A. thaliana* leaves, suggesting that other pathogenesis mechanisms, such as cell well degrading enzymes, are likely responsible for infection of this host.

Based on the present research, both host endogenous oxalate content and pathogen-produced OA affect interactions between *Clarireedia* sp. and its hosts. Results indicating that creeping bentgrass cultivars with resistance to dollar spot have lower oxalate levels than susceptible cultivars is the first indication that this physiological host characteristic is correlated with dollar spot resistance. Further studies on the relationship between oxalate content and resistance to dollar spot are needed, but this has potential as a quantifiable trait for selection of resistant clones in creeping bentgrass breeding programs. A limitation to our studies was the lack of genetic resources for *Clarireedia* sp. and one of its natural hosts, creeping bentgrass; however, we were able to identify potential model systems for study of *Clarireedia* sp./host interactions in this research. In the future, use of a model host system and development of functional genetic resources for *Clarireedia* sp. will enable elucidation of the importance of host oxalate and pathogen-produced OA for pathogenesis of this fungus.

Acknowledgements

We would like to thank the staff and students at the O.J. Noer Turfgrass Research and Education Facility for their efforts in this research. Thank you to the University of Wisconsin-Madison and Department of Plant Pathology for the support and oversight.

References

1. Kerns, J. P., and Tredway, L. P. Turfgrass: Biology, Use, and Management. American Society of Agronomy, Crop Science Society of America, Soil Science Society of America. 2013.
2. Salazar-Salgado C.; L. A. Beirn; A. Ismaiel; M. J. Boehm; I. Carbone; A.I. Putman; L. P. Treadway; B. B. Clarke; and J. A. Crouch. *Clarireedia*: A new fungal genus comprising four pathogenic species responsible for dollar spot disease of turfgrass. Fungal Biology. 2018; 122, 761-773.
3. Vu, A. L., Gwinn, K. D., and Ownley, B. H. First Report of Dollar Spot Caused by Sclerotinia homoeocarpa on Switchgrass in the United States. 2011.
4. Hoover, R. J. First Report of a Leaf Spot on Perennial Peanut Caused by Sclerotinia homoeocarpa. Plant Dis. 1995; 79:1249.
5. Hsiang, T., Shi, F., and Darbyson, A. First Report of Sclerotinia homoeocarpa from the Sedge Trichophorum cespitosum in Eastern Canada, Which Causes Dollar Spot Disease on Lolium perenne and Poa pratensis but not on Agrostis stolonifera. Plant Dis. 2014; 98:161–161.
6. Boland, G. J., and Hall, R. Index of plant hosts of Sclerotinia sclerotiorum. Can. J. Plant Pathol. 1994; 16:93–108.
7. Bolton, M. D., Thomma, B. P. H. J., and Nelson, B. D. Sclerotinia sclerotiorum (Lib.) de Bary: biology and molecular traits of a cosmopolitan pathogen. Mol. Plant Pathol. 2006; 7:1–16.
8. Bonos, S. A., and Huff, D. R. *Turfgrass: Biology, Use, and Management*. American Society of Agronomy, Crop Science Society of America, Soil Science Society of America. 2013.

9. Orshinsky, A. M., Hu, J., Opiyo, S. O., Reddyvari-Channarayappa, V., Mitchell, T. K., and Boehm, M. J. RNA-Seq Analysis of the Sclerotinia homoeocarpa – Creeping Bentgrass Pathosystem ed. Ying Xu. PLoS One. 2012; 7:e41150.
10. Chakraborty, N., Curley, J., Warnke, S., Casler, M. D., and Jung, G. Mapping QTL for dollar spot resistance in creeping bentgrass (Agrostis stolonifera L.). Theor. Appl. Genet. 2006; 113:1421–35.
11. Beneloujaephajri, E., Costa, A., L'haridon, F., Métraux, J.-P., and Binda, M. Production of reactive oxygen species and wound-induced resistance in Arabidopsis thaliana against Botrytis cinerea are preceded and depend on a burst of calcium. BMC Plant Biol. 2013; 13:160.
12. Dickman, M. B., and Mitra, A. Arabidopsis thaliana as a model for studying Sclerotinia sclerotiorum pathogenesis. Physiol. Mol. Plant Pathol. 1992; 41:255–263.
13. Guo, X., and Stotz, H. U. Defense against Sclerotinia sclerotiorum in Arabidopsis is dependent on jasmonic acid, salicylic acid, and ethylene signaling. Mol. Plant. Microbe. Interact. 2007; 20:1384–95.
14. Han, L., Li, G.-J., Yang, K.-Y., Mao, G., Wang, R., Liu, Y., and Zhang, S. Mitogen-activated protein kinase 3 and 6 regulate Botrytis cinerea-induced ethylene production in Arabidopsis. Plant J. 2010; 64:114–27.
15. Kabbage, M., Williams, B., and Dickman, M. B. Cell death control: the interplay of apoptosis and autophagy in the pathogenicity of Sclerotinia sclerotiorum. ed. Brett Tyler. PLoS Pathog. 2013; 9:e1003287.
16. Noyes, R. D., and Hancock, J. G. Role of oxalic acid in the Sclerotinia wilt of sunflower. Physiol. Plant Pathol. 1981; 18:123–132.

17. Krishnan, A., Guiderdoni, E., An, G., Hsing, Y. C., Han, C., Lee, M. C., Yu, S.-M., Upadhyaya, N., Ramachandran, S., Zhang, Q., Sundaresan, V., Hirochika, H., Leung, H., and Pereira, A. Mutant resources in rice for functional genomics of the grasses. Plant Physiol. 2009; 149:165–70.

18. Araneda, L., Sim, S.-C., Bae, J.-J., Chakraborty, N., Curley, J., Chang, T., Inoue, M., Warnke, S., and Jung, G. Comparative Genome Analysis between Agrostis stolonifera and Members of the Pooideae Subfamily, including Brachypodium distachyon ed. Giovanni G. Vendramin. PLoS One. 2013; 8:e79425.

19. Rotter, D., Bharti, A. K., Li, H. M., Luo, C., Bonos, S. a, Bughrara, S., Jung, G., Messing, J., Meyer, W. a, Rudd, S., Warnke, S. E., and Belanger, F. C. Analysis of EST sequences suggests recent origin of allotetraploid colonial and creeping bentgrasses. Mol. Genet. Genomics. 2007; 278:197–209.

20. Andrew, M., Barua, R., Short, S. M., and Kohn, L. M. Evidence for a common toolbox based on necrotrophy in a fungal lineage spanning necrotrophs, biotrophs, endophytes, host generalists and specialists. ed. Jason E. Stajich. PLoS One. 2012; 7:e29943.

21. Heller, A., and Witt-Geiges, T. Oxalic acid has an additional, detoxifying function in Sclerotinia sclerotiorum pathogenesis. PLoS One. 2013; 8:e72292.

22. Kim, K. S., Min, J.-Y., and Dickman, M. B. Oxalic acid is an elicitor of plant programmed cell death during Sclerotinia sclerotiorum disease development. Mol. Plant. Microbe. Interact. 2008; 21:605–12.

23. Bernier, F., and Berna, A. Germins and germin-like proteins: Plant do-all proteins. But what do they do exactly? Plant Physiol. Biochem. 2001; 39:545–554.

580 24. Van Loon, L. C., Rep, M., and Pieterse, C. M. J. Significance of inducible defense-related
581 proteins in infected plants. Annu. Rev. Phytopathol. 2006; 44:135–62.
582 25. Novak, L. A., and Kohn, L. M. Electrophoretic and Immunological Comparisons of
583 Developmentally Regulated Proteins in Members of the Sclerotiniaceae and Other
584 Sclerotial Fungi. Appl. Envir. Microbiol. 1991; 57:525–534.
585 26. Donaldson, P. A., Anderson, T., Lane, B. G., Davidson, A. L., and Simmonds, D. H. Soybean
586 plants expressing an active oligomeric oxalate oxidase from the wheat gf-2.8 (germin)
587 gene are resistant to the oxalate-secreting pathogen Sclerotina sclerotiorum. Physiol. Mol.
588 Plant Pathol. 2001; 59:297–307.
589 27. Dong, X., Ji, R., Guo, X., Foster, S. J., Chen, H., Dong, C., Liu, Y., Hu, Q., and Liu, S. Expressing
590 a gene encoding wheat oxalate oxidase enhances resistance to Sclerotinia sclerotiorum
591 in oilseed rape (Brassica napus). Planta. 2008; 228:331–40.
592 28. Hu, X., Bidney, D. L., Yalpani, N., Duvick, J. P., Crasta, O., Folkerts, O., and Lu, G.
593 Overexpression of a Gene Encoding Hydrogen Peroxide- Generating Oxalate Oxidase
594 Evokes Defense Responses in Sunflower. 2003; 133:170–181.
595 29. Orshinsky, A. M., Boehm, M. J., and Boland, G. J. Plant wounding and Ophiostoma mitovirus
596 3a (OMV3a) influence infection of creeping bentgrass by Sclerotinia homoeocarpa. Can.
597 J. Plant Pathol. 2012; 34:493–506.
598 30. Jia, Y., Liu, G., Park, D.-S., and Yang, Y. Inoculation and scoring methods for rice sheath
599 blight disease. Methods Mol. Biol. 2013; 956:257–68.
600 31. Horsfall, J. G., and Barratt, R. W. An improved grading system for measuring plant
601 diseases. Phytopathology. 1945; 35:655.

602 32. Chung, C.-L., Longfellow, J. M., Walsh, E. K., Kerdieh, Z., Van Esbroeck, G., Balint-Kurti, P.,
603 and Nelson, R. J. Resistance loci affecting distinct stages of fungal pathogenesis: use of
604 introgression lines for QTL mapping and characterization in the maize--Setosphaeria
605 turcica pathosystem. BMC Plant Biol. 2010; 10:103.
606 33. Ferrar, P. H., and Walker, J. R. L. O-Diphenol oxidase inhibition—an additional role for
607 oxalic acid in the phytopathogenic arsenal of Sclerotinia sclerotiorum and Sclerotium
608 rolfsii. Physiol. Mol. Plant Pathol. 1993; 43:415–422.
609 34. Bustin, S. A., Benes, V., Garson, J. A., Hellemans, J., Huggett, J., Kubista, M., Mueller, R., Nolan,
610 T., Pfaffl, M. W., Shipley, G. L., Vandesompele, J., and Wittwer, C. T. The MIQE guidelines:
611 minimum information for publication of quantitative real-time PCR experiments. Clin.
612 Chem. 2009; 55:611–22.
613 35. Hogan, C. S., Mole, B. M., Grant, S. R., Willis, D. K., and Charkowski, A. O. The type III
614 secreted effector DspE is required early in solanum tuberosum leaf infection by
615 Pectobacterium carotovorum to cause cell death, and requires Wx(3-6)D/E motifs. ed.
616 Stefan Bereswill. PLoS One. 2013; 8:e65534.
617 36. Pfaffl, M. W., Tichopad, A., Prgomet, C., and Neuvians, T. P. Determination of stable
618 housekeeping genes, differentially regulated target genes and sample integrity:
619 BestKeeper--Excel-based tool using pair-wise correlations. Biotechnol. Lett. 2004;
620 26:509–15.
621 37. Rotenberg, D., Thompson, T. S., German, T. L., and Willis, D. K. Methods for effective real-
622 time RT-PCR analysis of virus-induced gene silencing. J. Virol. Methods. 2006; 138:49–
623 59.
624 38. Conover, W. *Practical Nonparametric Statistics*. John Wiley & Sons. 1998.

625 39. Godoy, G., Steadman, J. R., Dickman, M. B., and Dam, R. Use of mutants to demonstrate the
626 role of oxalic acid in pathogenicity of Sclerotinia sclerotiorum on Phaseolus vulgaris.
627 Physiol. Mol. Plant Pathol. 1990; 37:179–191.
628 40. Massey, L. K., Palmer, R. G., and Horner, H. T. Oxalate Content of Soybean Seeds (Glycine
629 max : Leguminosae), Soyfoods, and Other Edible Legumes. J. Agric. Food Chem. 2001;
630 49:4262–4266.
631 41. Kawazu, Y., Okimura, M., Ishii, T., and Yui, S. Varietal and seasonal differences in oxalate
632 content of spinach. Sci. Hortic. (Amsterdam). 2003; 97:203–210.
633 42. Korth, K. L., Doege, S. J., Park, S.-H., Goggin, F. L., Wang, Q., Gomez, S. K., Liu, G., Jia, L., and
634 Nakata, P. A. Medicago truncatula mutants demonstrate the role of plant calcium oxalate
635 crystals as an effective defense against chewing insects. Plant Physiol. 2006; 141:188–95.
636 43. Yoshihara, T., Sogawa, K., Pathak, M. D., Juliano, B. O., and Sakamura, S. Oxalic acid as a
637 sucking inhibitor of the brown planthopper in rice (Delphacidae, homoptera). Entomol.
638 Exp. Appl. 1980; 27:149–155.
639 44. Libert, B., and Franceschi, V. R. Oxalate in crop plants. J. Agric. Food Chem. 1987; 35:926–
640 938.
641 45. Bonos, S. A., Casler, M. D., and Meyer, W. A. Inheritance of Dollar Spot Resistance in
642 Creeping Bentgrass. Crop Sci. 2003; 43:2189-2196.
643 46. Bonos, S. A., Casler, M. D., and Meyer, W. A. Plant Responses and Characteristics
644 Associated with Dollar Spot Resistance in Creeping Bentgrass. Crop Sci. 2004; 44:1763–
645 1769.
646 47. Bonos, S. A. Gene Action of Dollar Spot Resistance in Creeping Bentgrass. J. Phytopathol.
647 2011; 159:12–18.

48. Nelson, E. B., and Craft, C. M. Suppression of dollar spot on creeping bentgrass and annual bluegrass turf with compost-amended topdressings. Plant Dis. 1992; 76:954–958.

49. Goodman, D.M, and Burpee, L. L. Biological control of dollar spot. Phytopathology. 1991; 81:1438–1446.

50. Noyes, R. D., and Hancock, J. G. Role of oxalic acid in the Sclerotinia wilt of sunflower. Physiol. Plant Pathol. 1981; 18:123–132.

51. Rietz, S., Bernsdorff, F. E. M., and Cai, D. Members of the germin-like protein family in Brassica napus are candidates for the initiation of an oxidative burst that impedes pathogenesis of Sclerotinia sclerotiorum. J. Exp. Bot. 2012; 63:5507–19.

52. Zhou, T., and Boland, G. J. Mycelial growth and production of oxalic acid by virulent and hypovirulent isolates of Sclerotinia sclerotiorum. Can. J. Plant Pathol. 1999; 21:93–99.

53. Bennett, A. R., and Hindal, D. Mycelial growth and oxalate production by five strains of *Cryphonectria parasitica* in selected liquid culture media. Mycologia. 1989; 81:554–560.

Supporting Information

S1 Table. Plants used in this research.

S2 Table. Fungal isolates used in this research.

S3 Table. Symptom severity rating scale used for *Clarireedia* spp. infection of creeping bentgrass and models hosts.

S4 Table. Primers used for RT-qPCR expression analysis of creeping bentgrass GLP genes.

S1 Figure. Methods used for inoculation of various hosts with *Clarireedia* spp. A) Inoculation of *Arabidopsis thaliana* leaves with single agar plugs placed mycelia-side down on leaf surfaces. Inoculated plants were covered with a humidity dome to maintain high relative humidity. **B)** *Brachypodium distachyon* plants were inoculated by placing an agar plug colonized with *Clarireedia sp.* mycelium-side down against foliar material and wrapping with parafilm. **C)** Pots of creeping bentgrass were inoculated by collecting leaf blades in the center of the pot into a bundle and placing a single agar plug against the foliar tissue, then wrapping with parafilm. **D)** The most recent fully expanded leaf of barley, rice, and wheat plant were inoculated by placing a single agar plug colonized with *Clarireedia sp.* mycelia side down on the adaxial side of the leaf, then wrapping with parafilm. Mock-inoculations were performed similarly for all species but *Clarireedia sp.* colonized plugs were replaced with fresh PDA plugs.

S2 Figure. Oxalic acid production by *Clarireedia sp.* isolates. Oxalic acid production was measured *in vitro* using bromophenol blue amended medium, which changes from purple to yellow in color as a result of medium acidification. The area of color change was measured by averaging two perpendicular contrasts across the yellow areas. When areas of color change were diffuse, all were measured and the average measurements were combined. Columns represent the pooled means from three experimental repetitions with three replicates per isolate in each repetition (n=9).

684 Error bars represent ± one standard error of the mean. A1623 (red), ML75 (green), and HE10G14
685 (blue) were selected as isolates with high, moderate, and low oxalic acid production capacities,
686 respectively.

687 **S3 Figure. Selection of candidate oxalate oxidase and germin-like protein genes. A)** CRB
688 (AST) and representative barley (HvGer) and rice (Os) GLP amino acid sequences from rice and
689 barley were aligned using ClustalW. JalView was used to color sequence alignment according to
690 percent identity. Key features of GLP genes are annotated with green boxes and black text. Blue
691 arrowheads mark the start and end of the GLP cupin domain. 'AST' nucleotide sequences were
692 originally identified by Orshinsky et al. 2012. **B)** Maximum parsimony phylogenetic tree (100
693 bootstraps with sequence order re-arranging over 10 data sets) of CRB and select grass GLP- genes.
694 The percentage of replicate trees in which the associated taxa clustered together in the bootstrap
695 test are shown next to the branches. Rice and barley defense-associated GLP genes are indicated
696 by the green box. Oxalate oxidase-type CRB GLP-genes are indicated by the orange box. RT-
697 qPCR analysis of expression was performed for creeping bentgrass genes marked by an asterisk.
698 **C)** Time-course expression analysis for creeping bentgrass GLP-genes AST_590 and AST_608.
699 Both genes were significantly up-regulated in the *Clarireedia sp.*-inoculated susceptible cultivar
700 relative to the *Clarireedia sp.*-inoculated resistant cultivar and mock-inoculated susceptible
701 cultivar at 72 hpi ($P<0.05$). At 96 hpi, both genes were upregulated in the *Clarireedia sp.*-
702 inoculated susceptible and resistant cultivars relative to the mock-inoculated controls for each
703 cultivar ($P<0.05$). There was no difference in expression of either gene between the *Clarireedia*
704 *sp.*-inoculated susceptible and resistant cultivars at 96 hpi ($P>0.10$).

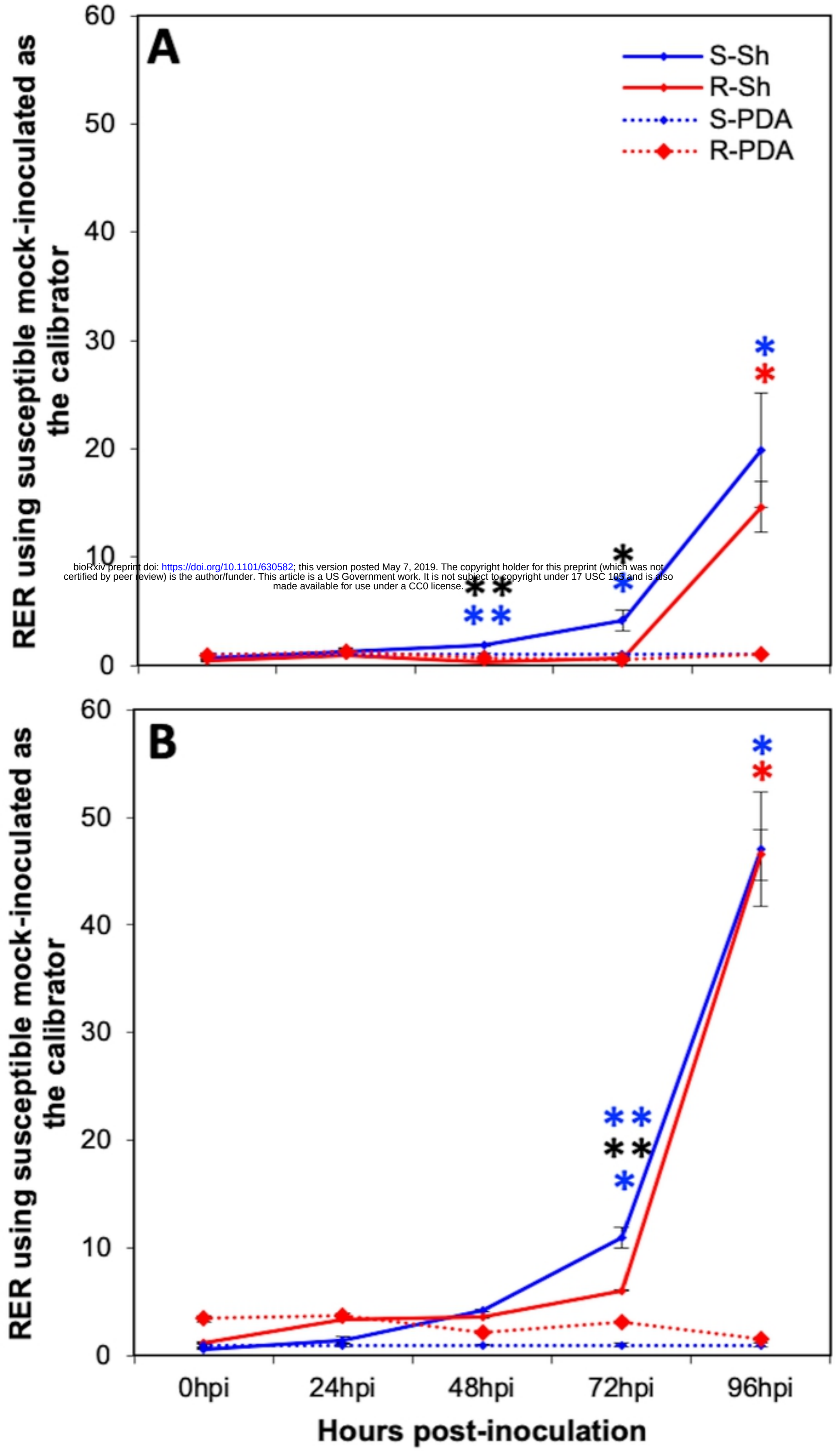

Figure 7

Figure 1

Figure 2

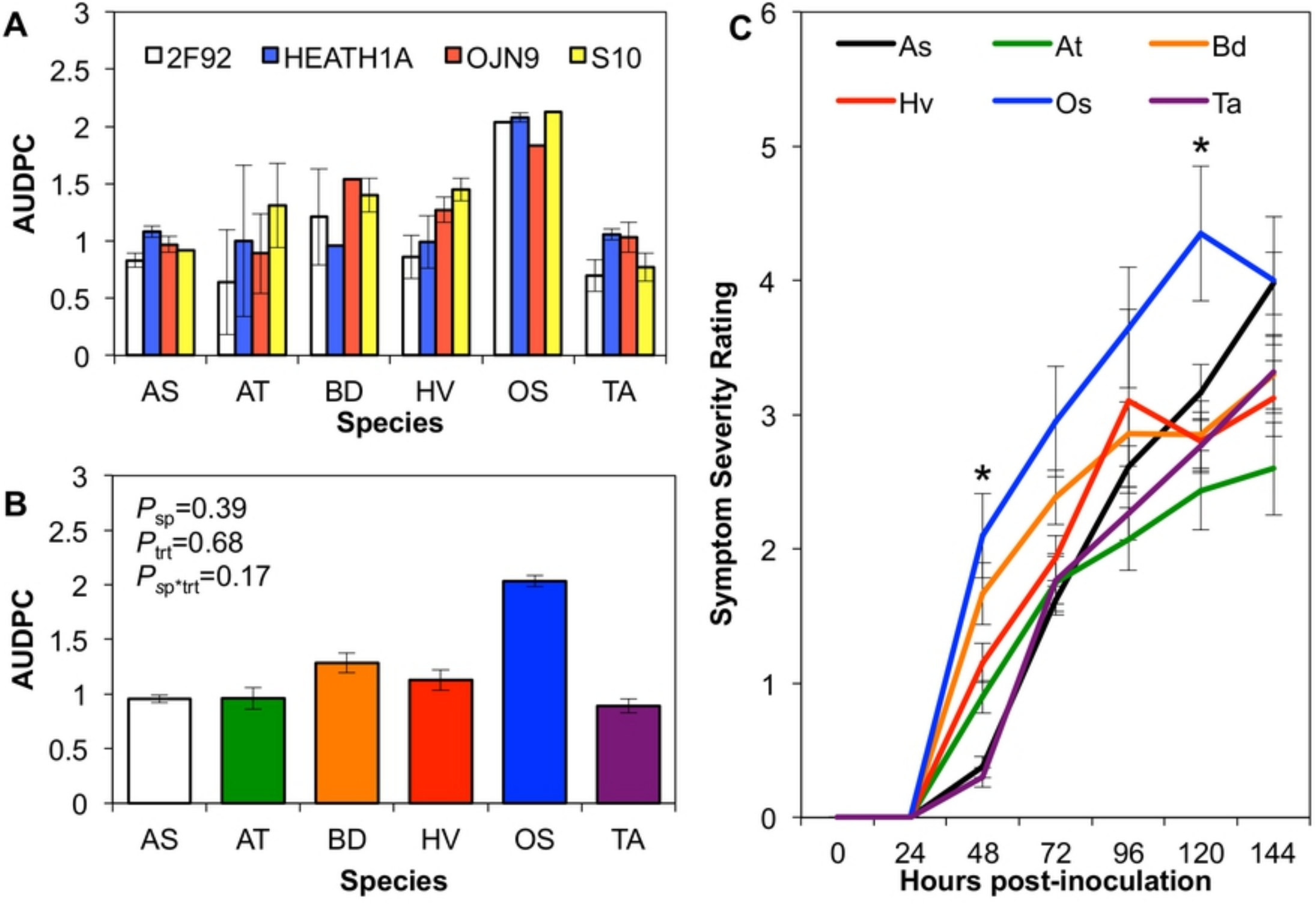
A
2F92
HEATH1A
OJN9
S10
AUDPC
Species
AS
AT
BD
HV
OS
TA
B
P_{sp}=0.39
P_{trt}=0.68
P_{sp*trt}=0.17
AUDPC
Species
C
As
At
Bd
Hv
Os
Ta
Symptom Severity Rating
Hours post-inoculation
*
*

Figure 3

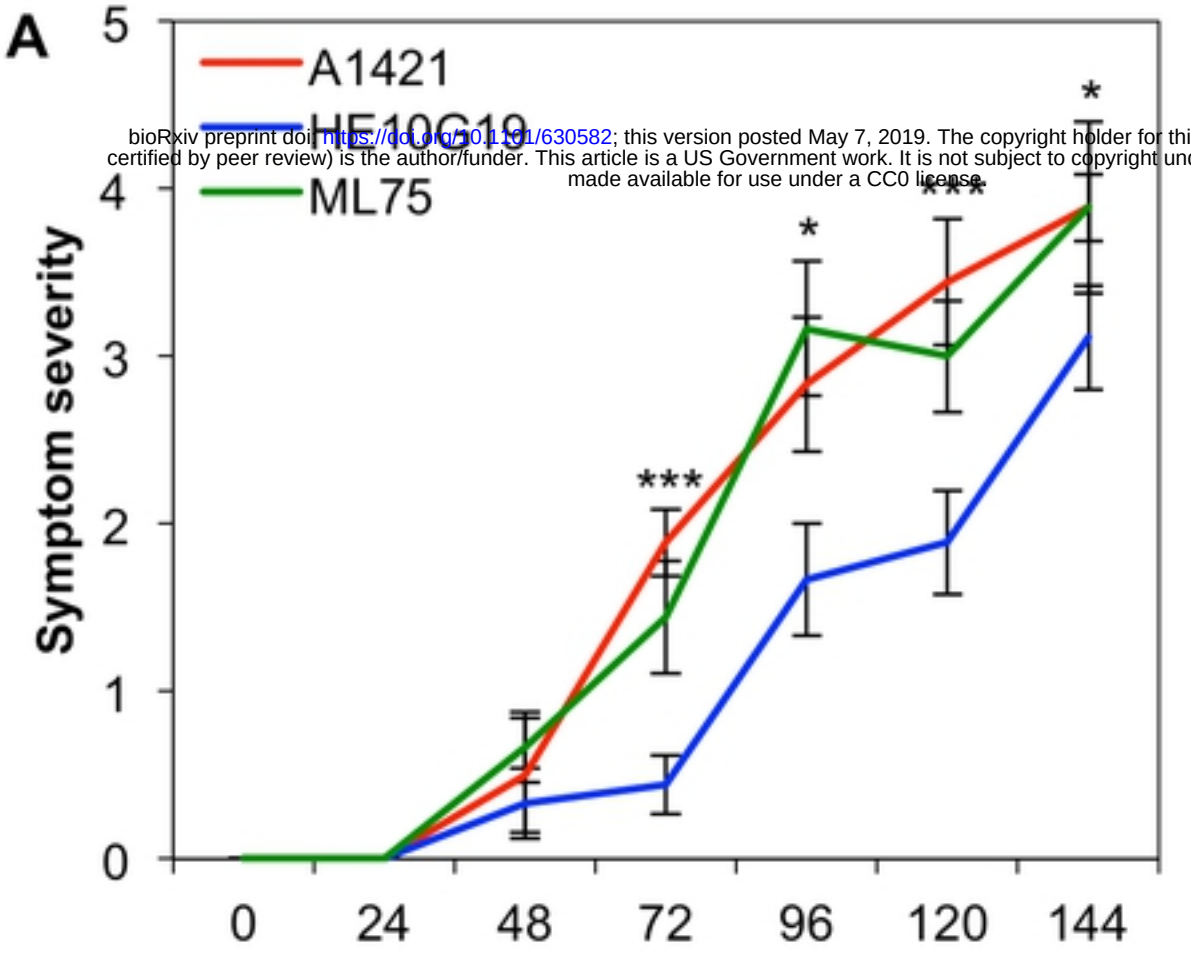

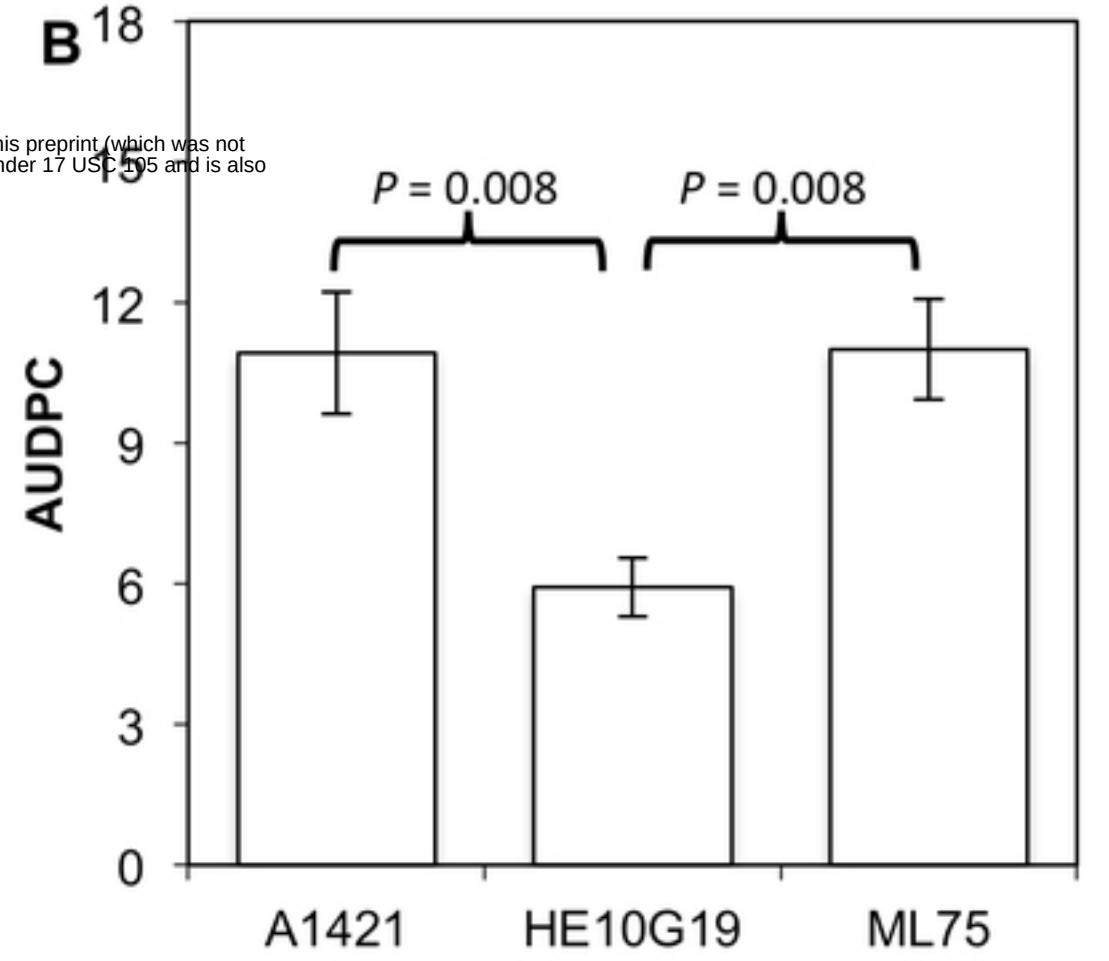

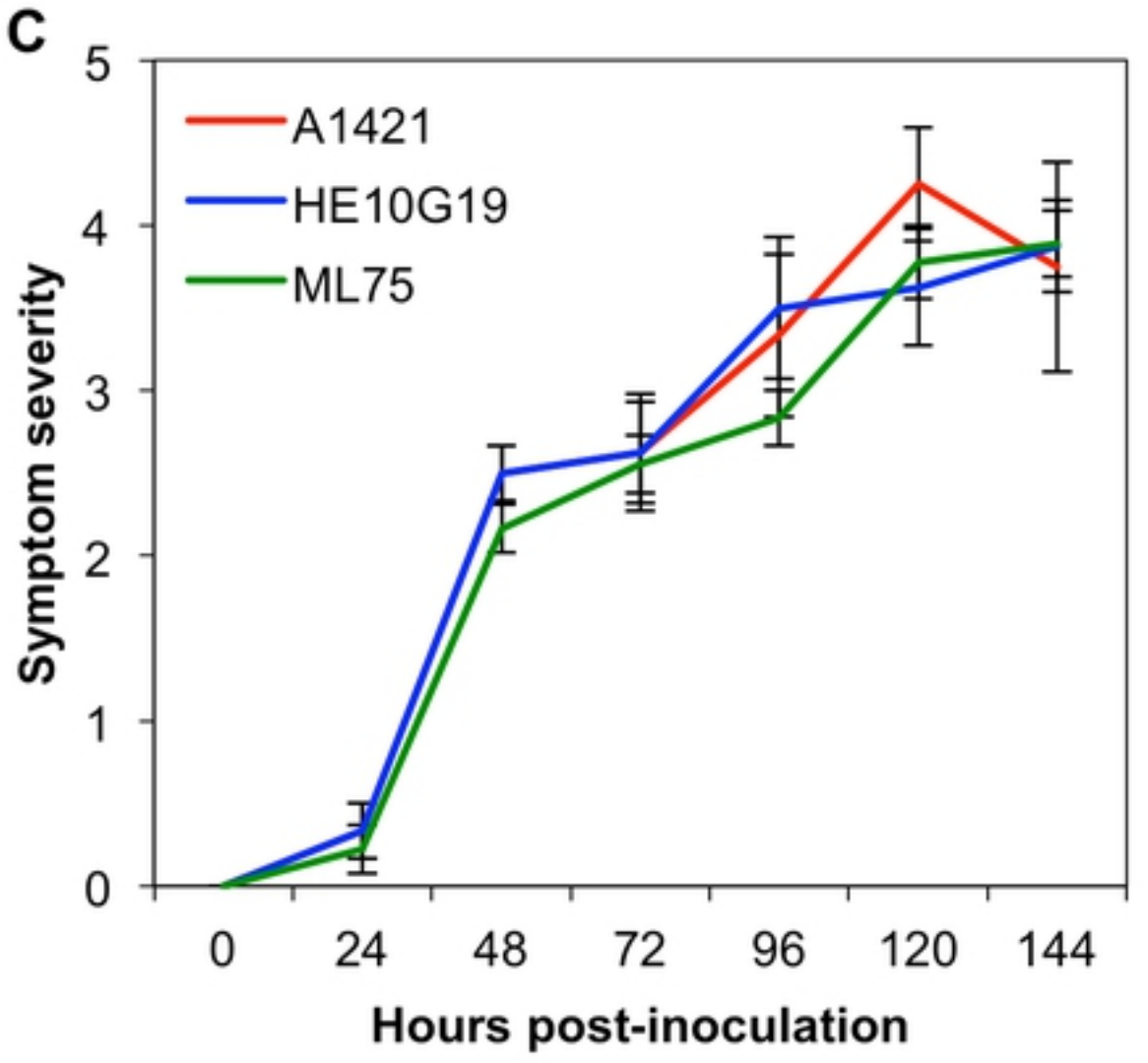

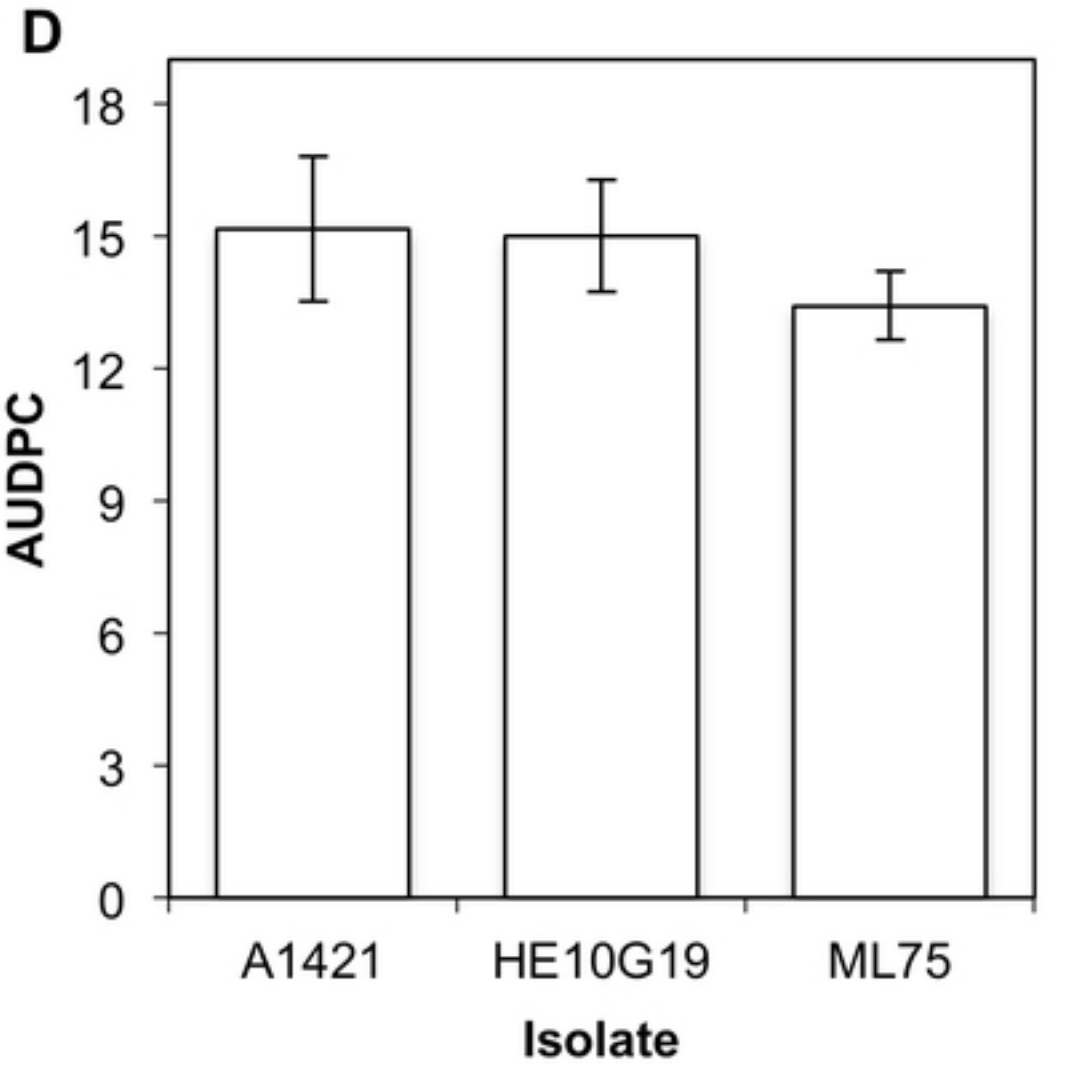

Figure 6

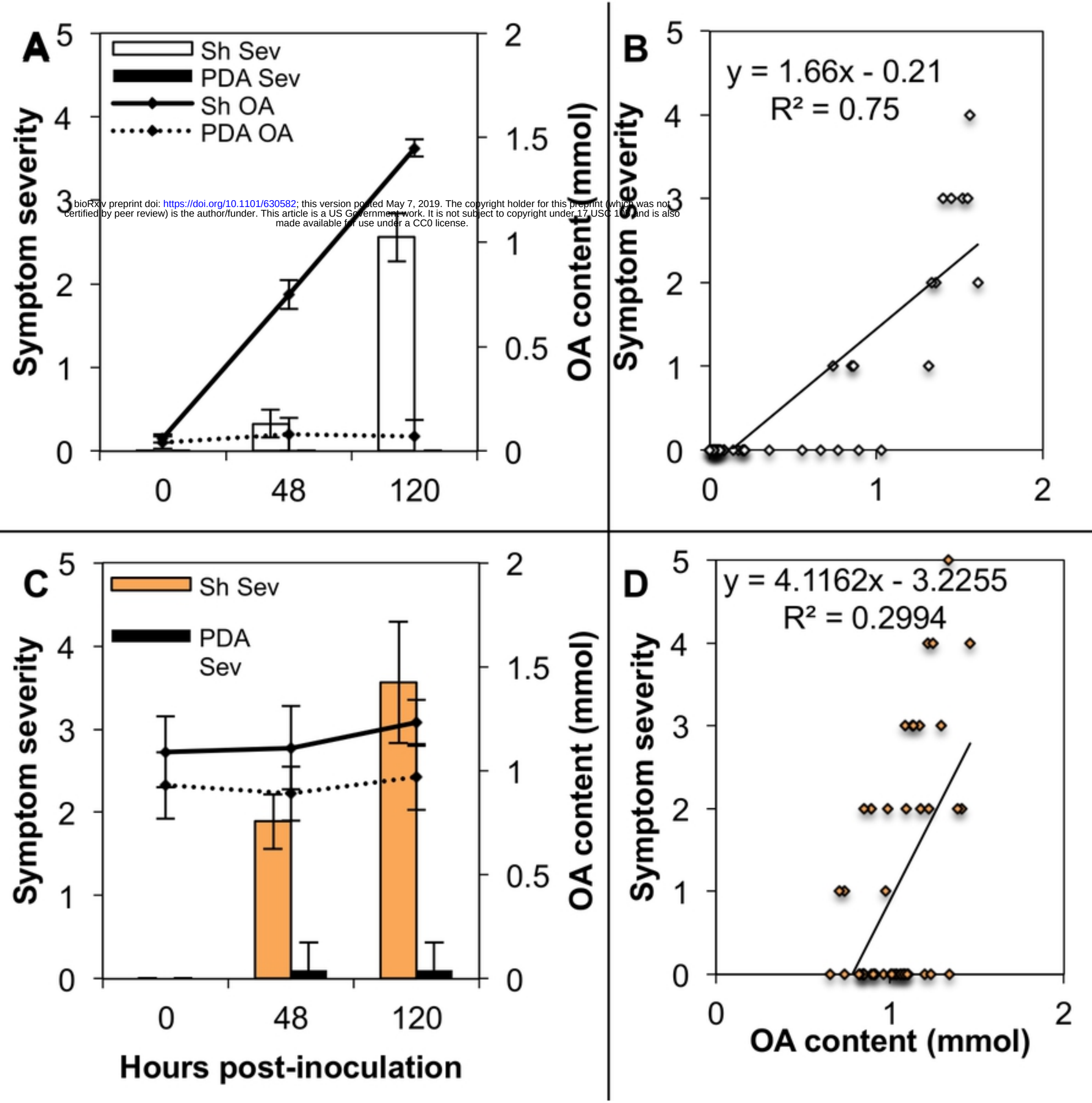

Figure 5

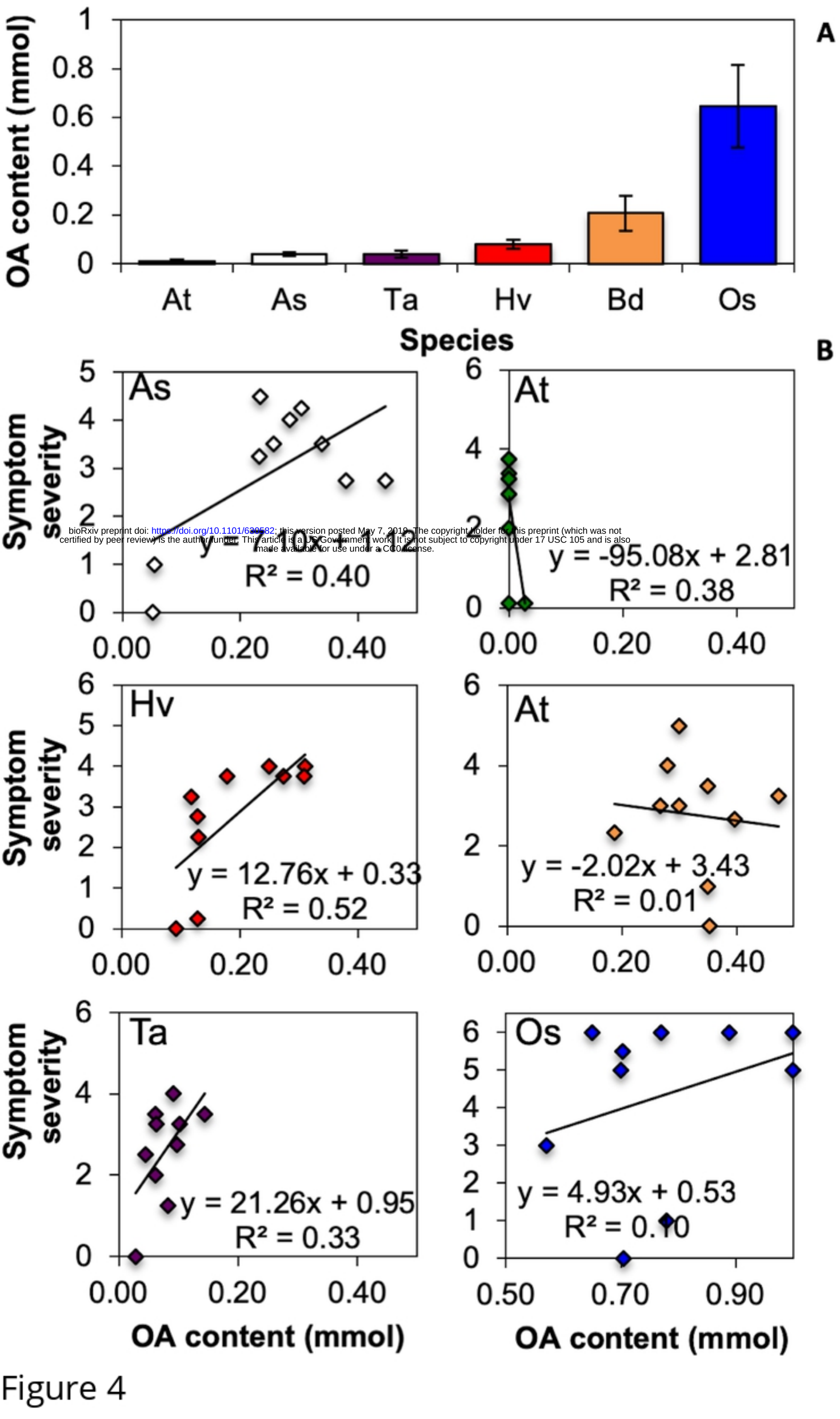

Figure 4